Australasian Physical & Engineering Sciences in Medicine (2019) 42:671–676
https://doi.org/10.1007/s13246-019-00764-3

SCIENTIFIC PAPER

Characterisation of out-of-field dose at shallow depths for external beam radiotherapy: implications for eye lens dose

Tina C. Baradaran[1] · Dean L. Cutajar[1,2] · Yujin Qi[1] · Anna Ralston[1,2]

Received: 24 December 2018 / Accepted: 16 May 2019 / Published online: 10 June 2019

Abstract

Re-evaluation of the eye lens radio-sensitivity by the ICRP in 2011 resulted in a significant reduction of the threshold for lens opacities from 8 Gy to 0.5 Gy. This has led to an increase in concern for eye lens doses from treatment sites further from the eye than previously considered. The aim of this study was to examine the out-of-field dose far from the field edge and develop an effective method to accurately characterise the constituent components of this dose at varying depths. Dose profile scans using a 0.6 cm^3 cylindrical ionisation chamber in a motorised water tank were compared with previous studies and displayed good agreement. At points more than 20 cm from the field edge patient scatter becomes insignificant, and the dose is dominated by head leakage and collimator scatter. Point depth-dose measurements made with a Roos parallel plate chamber in solid water at distances of 52 cm and 76 cm from central axis showed that the highest dose is at the surface. Since the sensitive region of the eye can be as shallow as 3 mm, in vivo measurements carried out with a detector with buildup more than 3 mm water equivalent thickness may be underestimating the dose to the lens. It is therefore recommended that for in vivo measurements for the eye lens further than 20 cm from the field edge the detector should have only 3 mm build-up material over the effective point of measurement.

Keywords Eye lens dose · Out-of-field dose · Head leakage · Collimator scatter · Patient scatter · Shallow depths

Introduction

The principle goal of radiation therapy is to maximise the dose delivered to a well-defined treatment volume, while minimising the dose spreading into surrounding healthy tissues and organs, with the aim of eradicating the disease, prolonging the life and/or improving the quality of life of the patient. However, external beam radiation therapy also brings an unavoidable out-of-field dose to the patient. Although the magnitude of the out-of-field dose is relatively small compared to the prescribed target dose, it could cause a significant radiobiological effect to the critical organs/tissues such as the eye lens. The International Commission on Radiological Protection (ICRP) reviewed epidemiological evidence for the late effects of radiation induced damage. In 2011 the ICRP then issued a statement on tissue reactions containing a series of recommendations including a revision of the eye lens limit, lowering the threshold for eye lens opacities from the previous 8 Gy to 0.5 Gy [1].

As cancer patients are tending to live longer after initial diagnosis and treatment, there is increased potential for late effects including secondary cancers [2] and cardiac toxicity to manifest [3]. To develop an accurate and comprehensive out-of-field risk model for cancer patients, there are many challenges involved [4]. Out-of-field dose is a result of leakage from the treatment head and scatter arising from collimation devices and patient scatter. It varies largely with treatment type and parameter setting. Therefore, there is a large difficulty in predicting and determining the out-of-field dose accurately.

Currently, there are a few options available to determine the out-of-field dose. The most straightforward one is measuring the dose to the patient, however these measurements are time consuming, yield only the dose to the specific measured points and are specific to the particular treatment and patient examined. Radiotherapy treatment planning systems (TPS) are not commissioned or designed for out-of-field

✉ Tina C. Baradaran
tb280@uowmail.edu.au

[1] Centre for Medical Radiation Physics, University of Wollongong, Wollongong, NSW, Australia

[2] St George Cancer Care Centre, St George Hospital, Kogarah, NSW, Australia

dose calculations [5]. Although most treatment planning systems can display the dose at points far from the treatment field, they do not accurately model radiation leakage or scatter from the linear accelerator (linac) head [6–9]. Several studies [6, 9, 10] reported that the analytic or model-based algorithms in commercial TPS significantly underestimate the true out-of-field dose. Monte Carlo simulation-based calculations can provide accurate out-of-field dose estimation [11]. Estimates of out-of-field doses are given in the AAPM Task Group 36 report [12], however these were for fetal doses at depths of at least 2 cm and are not relevant to the case of eye lens.

Early studies by Starkschall et al. [13] have found that the out-of-field dose varies minimally with depth in the patient, except near the surface. Studies by Kry et al. [14] and Ruben et al. [15] have further explored out-of-field dose at shallow depths, however the shallowest depths investigated were only 3.75 cm and 10.0 cm respectively. AAPM Task Group 158 was formed to provide guidance for assessing and managing non-target doses. The report developed by this task group [16] provides a rough estimate of doses associated with different treatment approaches in clinical practice, however it does not investigate out-of-field dose close to the surface. Kry et al. [17] examined skin dose during radiotherapy and found that outside the treatment field the skin dose was highly elevated, relative to the dose at depth in the patient. Recent measurements by Peet et al. [18] from radiotherapy treatments in the vicinity of a cardiac pacemaker at depths as shallow as the skin 5 mm showed that the skin dose was two to three times greater than the dose at the depth of the device. Therefore, validation of out-of-field dose near the surface especially at depths shallower than the beam's maximum build-up region, d_{max} need to be examined, as the dose near the surface is substantially elevated by electrons.

The aim of this study was to develop a reliable experimental method to measure and examine the out-of-field doses at shallow depths under a range of varying conditions with changing distance, depth, collimator angle, jaw-defined field size and MLC field size. This method can be used to examine the dose to the sensitive cells of the eye lens, which have been estimated to be at a depth of 2–4 mm [4] as illustrated in Fig. 1.

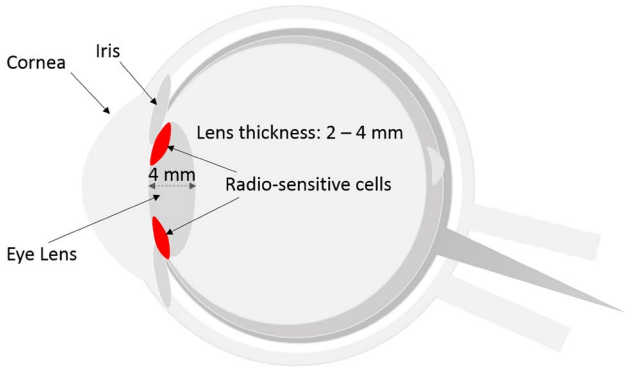

Fig. 1 Schematic diagram of the eye representing the radio-sensitive region of the eye lens

Methods and materials

Calibrating the output of the common linac (Varian iX) photon beam with the Roos and 0.6 cm^3 ionisation chamber, was done in RMI solid water, to generate the calibration coefficients for the 6 MV beam. This was achieved by setting the linac to reference conditions: gantry angle 0°, collimator angle 0°, Focus to Source Distance = 100 cm, jaw-defined field size of 10 cm × 10 cm and MLCs retracted at 40 cm × 40 cm. The Roos and 0.6 cm^3 ionisation chamber (PTW Freiburg, TM31010) was set at a voltage of 150 V, with a PTW UNIDOS® T10001-11678 electrometer measuring the capacitor charging current. The Roos and 0.6 cm^3 cylindrical ionisation chamber were placed at isocentre and 100 MU was delivered to the chamber in solid water at an effective depth of d_{max} = 15 mm the chamber calibration coefficients were essential to convert the reading measurements from charge (pC) to dose (μGy/MU) in non-reference conditions.

The initial out-of-field profile scans were performed to reproduce the set-up of Kry et al. [14]. The 0.6 cm^3 cylindrical chamber was positioned at depths of 37.5 mm and 112.5 mm, as they were the effective points of measurements accounted for in Kry et al. [14] setup, with the scan ranges set to 15–70 cm away from the central axis. Solid water sheets were placed in the beam to provide phantom scatter. The dose profile measurements were compared to the results of Kry et al. [14] to verify the study's experimental methods.

Out-of-field depth dose measurements were performed with a Roos parallel plate chamber in RMI solid water at various distances from central axis to get percentage depth dose data, at depths ranging from 1 to 15 mm. Two distances of out-of-field locations of the eye lens were selected at 76 cm and 52 cm from the central axis to be carefully examined. The distance of 76 cm was selected as it was the best estimate of the distance from a prostate treatment to the eye lens and the second distance of 52 cm was selected as it was a point that would simulate a target closer to the eye lens. The Roos chamber was chosen as it provides good spatial resolution in the depth direction and reasonable efficiency for low-current signal (pC) measurements. The out-of-field depth dose measurements were taken at gantry angle of 0°, collimator angle 0°, and at three different jaw-defined field sizes: 0.5 cm × 0.5 cm, 10 cm × 10 cm and 20 cm × 20 cm and with the MLCs retracted at 40 cm × 40 cm.

Out-of-field dose profile scans were made in a 73.4 cm × 63.6 cm × 52.3 cm PTW MP3 motorised water tank, with a source-to-surface distance (SSD) of 90 cm and gantry angle 0°. The tank was controlled by MEPHYSTO® mc^2 software and the scan parameters were set to obtain optimal results for the very low dose rates encountered at the out-of-field positions. The scans were taken on low range settings and with a dwell time of 1 s at each position, ten times greater than for in-field measurements which are generally 0.1 s or less. The step size was 2 mm between 170 and 300 mm from the beam central axis and 20 mm from 300 to 750 mm from the beam central axis. A detector with high sensitivity and minimal angular dependence was required for measuring the very low current (pC), therefore a 0.6 cm^3 waterproof cylindrical ionisation chamber (PTW Freiburg, TM31010) was used, which has a volume of nearly five times that of a standard 0.125 cm^3 scanning ionisation chamber. The water tank was positioned to be just outside the field edge so that the phantom scatter could be excluded when required, as shown in Fig. 2. An anthropomorphic pelvis phantom or a stack of solid water sheets was placed under the beam as scatter material when measurements included phantom scatter.

Further water tank dose profile scans were performed to characterise the out-of-field dose components and examine their relative contributions. To separate the constituent components of head leakage (HL), collimator scatter (CS) and internal patient scatter (PS), dose profiles were performed 20 cm away from the central axis up until 70 cm, at depths of 5 mm, 15 mm and 37.5 mm. The source to water surface distance (SSD) was set to 90 cm. The experimental set-up is shown in Fig. 2. Two types of experiments were performed as follows.

Total dose including head leakage (HL) + collimator scatter (CS) + patient scatter (PS)

The total scattered contribution from HL, CS and PS was obtained by performing scans at gantry angle 0°, at collimator angle 0° and 270°, jaw-defined field size of 10 cm × 10 cm and MLC field size of 10 cm × 10 cm. An anthropomorphic pelvis phantom was placed directly under the treatment beam to provide phantom scatter. Separate scans were performed for each set of conditions to compare the different collimator angle 0° and 270°, at varying depths.

$$Total\ dose = HL + CS + PS$$

Head leakage (HL) + collimator scatter (CS)

To measure the contribution of scattered radiation from head leakage and collimator scatter alone, the pelvic phantom was removed from isocentre, out of the treatment beam. The primary beam did not pass through the water in the tank, eliminating the contribution of phantom scatter. The scans were performed at gantry angle 0°, at collimator angle 0° and 270°, jaw-defined field size of 10 cm × 10 cm and MLC field size of 10 cm × 10 cm. Scans were performed for collimator angle 0° and 270°, at varying depths. To measure the contribution of scattered radiation from head leakage alone, collimator scatter had to be blocked, however this was not practically achievable with our equipment.

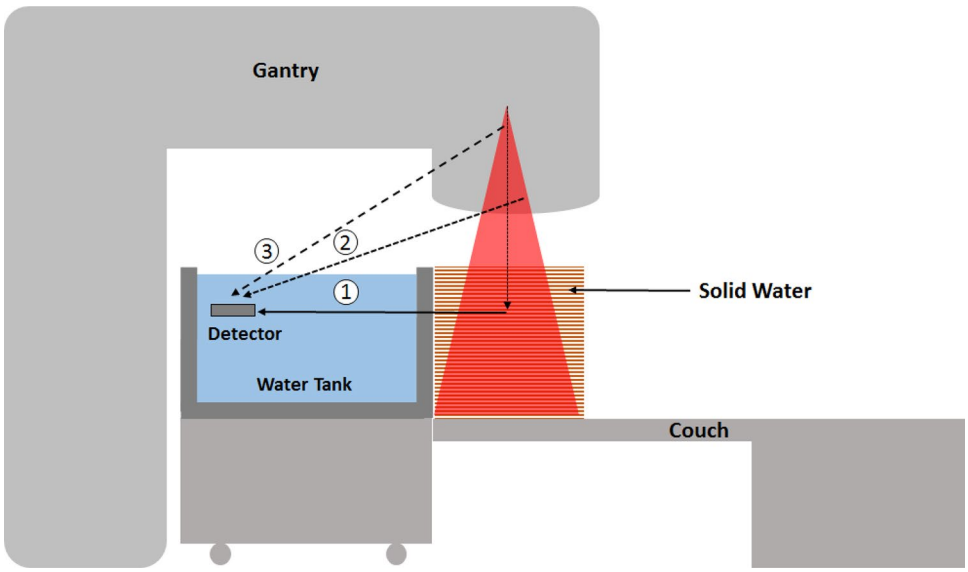

Fig. 2 Experimental set-up showing the sources of out-of-field dose from a medical linear accelerator: (*1*) patient scatter, (*2*) secondary collimator scatter, and (*3*) head leakage

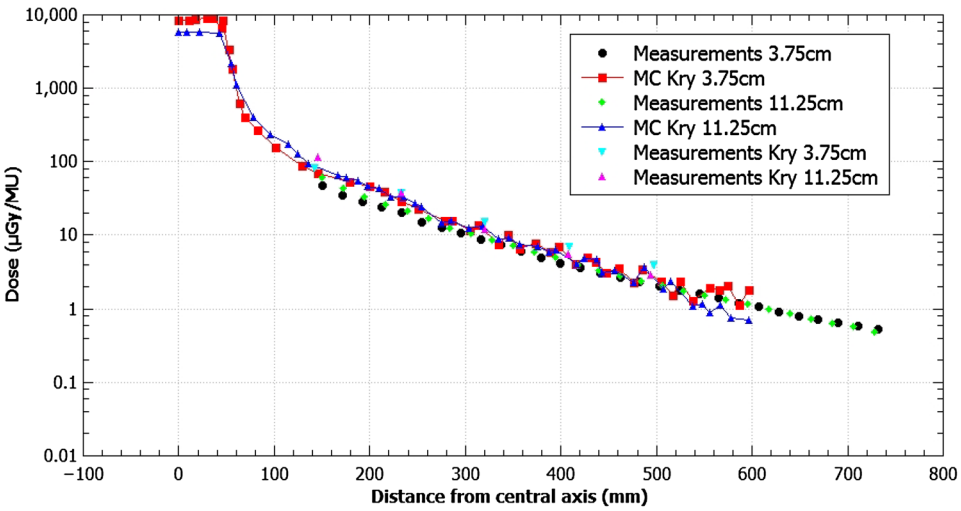

Fig. 3 Out-of-field dose profiles as a function of distance from the central axis at depths 3.75 cm and 11.25 cm, with a jaw-defined field size of 10 cm × 10 cm, compared to both measurements and Monte Carlo simulations from Kry et al. [14]

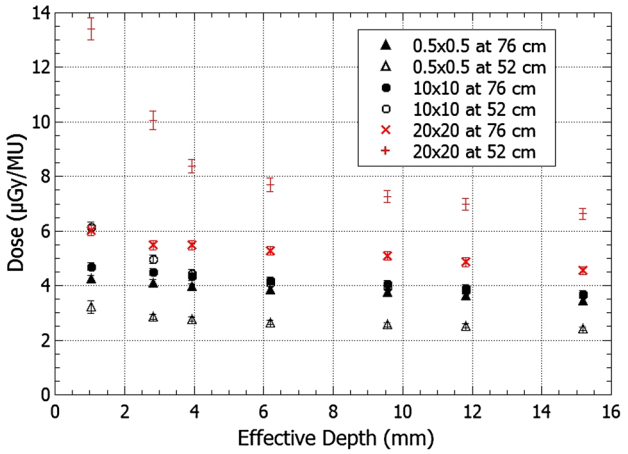

Fig. 4 Out-of-field point depth dose measurements using a Roos chamber in solid water, at distances of 52 cm and 76 cm from central axis, with jaw-defined field sizes of 0.5 cm × 0.5 cm, 10 cm × 10 cm and 20 cm × 20 cm

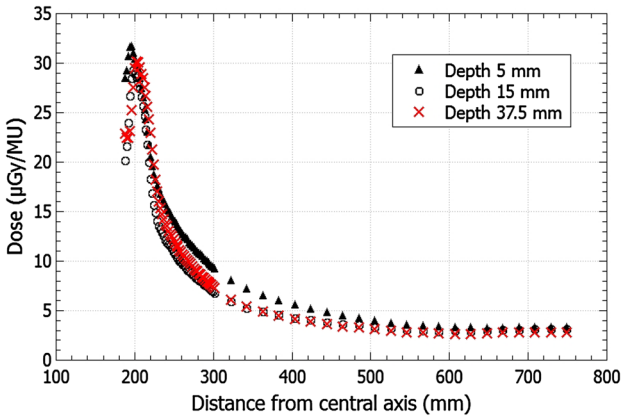

Fig. 5 Total scatter contribution using a 0.6 cm^3 cylindrical chamber at collimator 0°, jaw-defined field size of 10 cm × 10 cm and MLC field size 10 cm × 10 cm. Maximum uncertainty 6% (95% confidence interval)

Results

The validation results of out-of-field dose profiles in a water tank, at depth of 3.75 cm and 11.25 cm, with a jaw-defined field size of 10 cm × 10 cm are shown in Fig. 3, with the water tank scan measurements compared with published measurements and Monte Carlo simulations from Kry et al. [14].

Figure 4 displays the point depth dose measurements at 52 cm and 76 cm from central axis, with jaw-defined field sizes of 0.5 cm × 0.5 cm, 10 cm × 10 cm and 20 cm × 20 cm, at depths ranging from 1 to 15 mm. The depth dose curves show the dose to be greater near the surface, and greater for larger jaw-defined field sizes. For the 20 cm × 20 cm jaw-defined field size the dose at 52 cm from central axis was roughly double that at 76 cm. For the smaller jaw-defined field size of 0.5 cm × 0.5 cm the opposite trend is noted, whereby the dose at 52 cm from central axis is less than that 76 cm from central axis. For the 10 cm × 10 cm jaw-defined field size the dose is similar at both points.

Figure 5 illustrates the water tank scans of total scattered contribution from all sources at collimator angle 0°, and depths of 5 mm, 15 mm and 37.5 mm. Figure 6 displays the head leakage and collimator scatter alone without the presence of patient scatter. At collimator angle 0°, both Figs. 5 and 6 display a prominent peak at approximately 20 cm from the central axis.

Figure 7 illustrates the water tank scans of total scattered contribution from all sources at collimator angle 270°, and depths of 5 mm, 15 mm and 37. 5 mm. Figure 8 displays the head leakage and collimator scatter alone without the

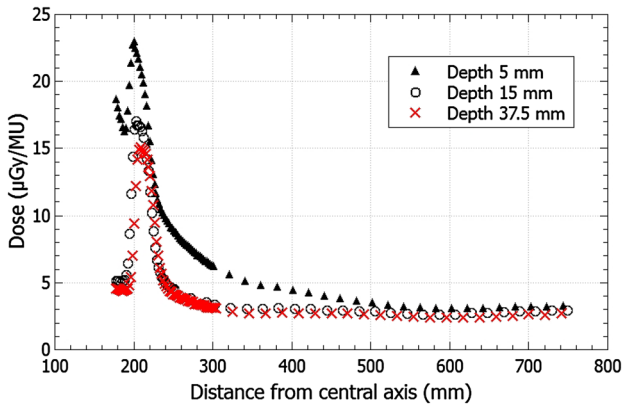

Fig. 6 Head leakage + collimator scatter using a 0.6 cm^3 cylindrical chamber at collimator 0°, jaw-defined field size of 10 cm × 10 cm and MLC field size 10 cm × 10 cm. Maximum uncertainty 6% (95% confidence interval)

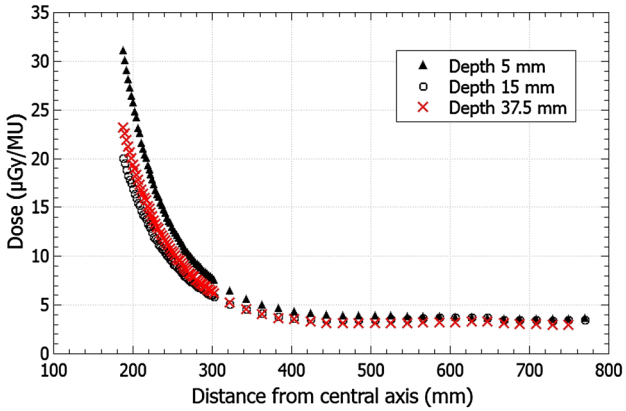

Fig. 7 Total scatter contribution using a 0.6 cm^3 cylindrical chamber at collimator 270°, jaw-defined field size of 10 cm × 10 cm and MLC field size 10 cm × 10 cm. Maximum uncertainty 6% (95% confidence interval)

presence of patient scatter. At collimator angle 270°, both Figs. 7 and 8 do not display the peak shown in Figs. 5 and 6. Similar results were observed for collimator angle 45°.

Discussion

The dose profile scans outside a 6 MV photon beam, at depths of 3.75 cm and 11.25 cm, were validated with the measured and Monte Carlo results of Kry et al. [14]. This indicates that our established measuring method and system are effective and reliable for the out-of-field dose measurements.

The solid water point dose measurements at depths ranging from 1 to 15 mm (Fig. 4) show that the highest

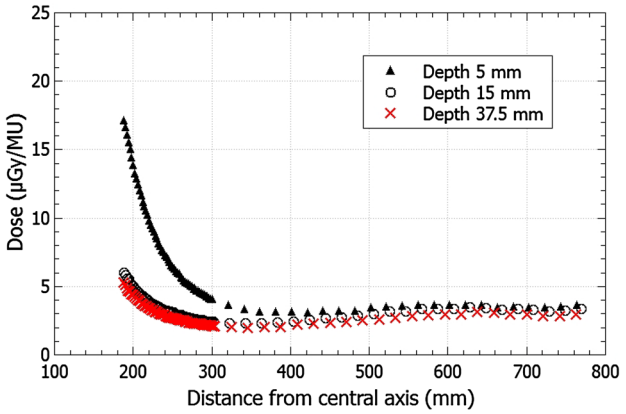

Fig. 8 Head leakage + collimator scatter using a 0.6 cm^3 cylindrical chamber at collimator 270°, jaw-defined field size of 10 cm × 10 cm and MLC field size 10 cm × 10 cm. Maximum uncertainty 6% (95% confidence interval)

dose is at the shallowest depth, which is mostly due to electron contamination [4, 14]. These findings of the surface dose being the highest are also supported by Peet et al. [18] in a recent study of the out-of-field dose in the vicinity of a cardiac pacemaker. This is important, as the sensitive region of the eye lens where radiation becomes of critical concern is between 2.8 and 3.8 mm and therefore will be adversely affected by the high doses near the surface.

The observed phenomenon in Fig. 4, a higher leakage dose exhibiting in the small field size at the greater distance than at the closer distance, is likely due to the radiation shielding geometry changing between the jaws and the general head shielding associated with the field sizes.

Figures 5 and 6 show that for collimator angle 0°, there is a prominent peak at approximately 20 cm from the central axis. This is in good agreement with the findings of Constantin et al. [19], who used Monte Carlo modeling to show that this peak is due to scattered radiation generated in the primary collimator and flattening filter travelling past the outermost leaves of the MLC bank, in the direction perpendicular to the direction of leaf travel. In contrast to the measurements at collimator 0°, at collimator angle 270° both Figs. 7 and 8 do not display a dose peak at approximately 20 cm from the central axis. This is expected as the tails of the MLC leaves provide shielding further from the central axis in the direction of the leaf travel, compared to the perpendicular direction.

Overall, total scattered radiation dose and the constituent components of out-of-field dose, head leakage and collimator scatter together were successfully characterised. The total scatter contributions would also vary with beam energy, treatment mode (static beams, IMRT or VMAT) and internal components within the linac, as the contributions of

head leakage and collimator scatter are dependent on linear accelerator and collimator design [16].

Notably, for patients where the dose to the eye lens is of critical concern, or where the treated volume is close to the area at risk, the dose should be measured either in vivo or in a phantom. Traditionally, eye lens doses have been measured in vivo using MV photon detectors with water equivalent build-up of 5–15 mm, for example, silicon detectors with in-built metal build-up caps, or OSLDs and TLDs with plastic, wax or wet gauze build-up even though the radiosensitive region of the eye lens can be as shallow as 3 mm. This study has shown that the out-of-field doses are highest at the surface and fall off with depth, so in vivo measurements carried out with a detector deeper than 3 mm may be underestimating the dose to the lens. It is therefore recommended that in vivo detectors have a 3 mm build up for estimating dose to the radiosensitive cells of the eye, particularly when used closer than 20 cm from the field edge.

Conclusion

In this study, we have successfully evaluated the out-of-field dose at shallow depths in the dose sparing region far from the radiation field edge in a common linac (Varian iX) operated at 6 MV. Under the conditions tested, more than 20 cm from the field edge patient scatter becomes insignificant, and the dose is dominated by head leakage and collimator scatter. In this region, the highest dose is at the surface, which is mostly due to electrons. Since the sensitive region of the eye lens can be as shallow as 3 mm, in vivo measurements carried out with the detector deeper than 3 mm may be underestimating the dose to the lens. It is therefore recommended that for in vivo measurements for the eye lens further than 20 cm from the field edge the detector should have only 3 mm water equivalent build-up material over the effective point of measurement.

Compliance with ethical standards

Conflict of interest We the authors confirm there is no conflict of interest and no human/animal testing involved in this research.

References

1. International Commission on Radiological Protection (ICRP) (2011) Statement on tissue reactions. Tech Rep
2. Harrison R (2017) Out-of-field dose in radiotherapy: input to epidemiological studies and dose-risk models. Phys Med 42:239–246
3. Mulrooney DA, Yeazel MW, Kawashima T, Mertens AC, Mitby P, Stovall M, Donaldson SS, Green DM, Sklar CA, Robison LL, Leisenring WM (2009) Cardiac outcomes in a cohort of adult survivors of childhood and adolescent cancer: retrospective analysis of the Childhood Cancer Survivor Study cohort. Br Med J. https://doi.org/10.1136/bmj.b4606
4. Behrens R, Dietze G, Zankl M (2009) Dose conversion coefficients for electron exposure of the human eye lens. Phys Med Biol 54(13):4069–4087
5. Das IJ, Cheng C (2008) Accelerator beam data commissioning equipment and procedures: report of the TG-106 of the Therapy Physics Committee of the AAPM. Med Phys 35(9):4186–4215
6. Howell RM, Scarboro SB, Kry SF, Yaldo DZ (2010) Accuracy of out-of-field dose calculations by a commercial treatment planning system. Phys Med Biol 55(23):6999–7008
7. Joosten F, Bochud S, Baechler F, Levi R-O, Mirimanoff R, Moeckli R (2011) Variability of a peripheral dose among various linac geometries for second cancer risk assessment. Phys Med Biol 56:5131–5151
8. Joosten O, Matzinger W, Jeanneret-Sozzi F, Bochud R, Moeckli R (2013) Evaluation of organ-specific peripheral doses after 2-dimensional, 3-dimensional and hybrid intensity modulated radiation therapy for breast cancer based on Monte Carlo and convolution/superposition algorithms: implications for secondary cancer risk asses. Radiother Oncol 106(1):33–41
9. Huang JY, Followill DS (2013) Accuracy and sources of error of out-of field dose calculations by a commercial treatment planning system for intensity modulated radiation therapy treatments. J Appl Clin Med Phys 14(2):186–197
10. Heuvel FVD, Defraene G, Crijns W, Bogaerts R (2012) Out-of-field contributions for IMRT and volumetric modulated arc therapy measured using gafchromic films and compared to calculations using a superposition/convolution-based treatment planning system. Radiother Oncol 105:127–132
11. Wang L, Ding GX (2014) The accuracy out-of-field dose calculations using a model based algorithm in a commercial treatment planning system. Phys Med Biol 59:N113–N128
12. Stovall M, Blackwell CR, Cundiff J, Novack DH, Palta JR, Wagner LK, Webster EW, Shalek RJ (1995) Fetal dose from radiotherapy with photon beams: report of AAPM radiation therapy committe task group. 36. Med Phys 22(1):63–82
13. Starkschall G, St George FJ, Zellmer DL (1983) Surface dose for megavoltage photon beams outside the treatment field. Med Phys 10(6):906–910
14. Kry SF, Titt U, Ponisch F, Followill D, Vassiliev ON, White RA, Mohan R, Salehpour M (2006) A Monte Carlo model for calculating out-of-field dose from a Varian 6 MV beam. Med Phys 33(11):4405–4413
15. Ruben JD, Lancaster CM, Jones P, Smith RL (2011) A comparison of out-of- field dose and its constituent components for intensity-modulated radiation therapy versus conformal radiation therapy: implications for carcinogenesis. Int J Rad Oncol Biol Phys 81(5):1458–1464
16. Kry SF, Bednarz B, Howell RM, Dauer L, Followill D, Klein E, Paganetti H, Wang B, Wuu C-S, Xu X (2017) AAPM TG 158 measurement and calculation of doses outside the treated volume from external-beam radiation therapy. Med Phys 44(10):e391–e429
17. Kry SF, Smith SA, Weathers R, Stovall M (2012) Skin dose during radiotherapy: a summary and general estimation technique. J Appl Clin Med Phys 13(3):20–34
18. Peet SC, Wilks R, Kairn T, Crowe SB (2016) Measuring dose from radiotherapy treatments in the vicinity of a cardiac pacemaker. Phys Med 32(12):1529–1536
19. Constantin M, Hsu H, Mansfield S, Svatos M (2013) Mitigation strategies to reduce the relative extrafocal dose (RED). Med Phys 40(6):322